Aerodynamic stability of Suramadu cable stayed bridge

Sukamta*, Fumiaki Nagao**, Minoru Noda*** and Kazuyuki Muneta****

*M. of Eng., Graduate student, The University of Tokushima, 2-1, Minami-Josanjima, Tokushima, 770-8506
**Dr. of Eng., Professor, The University of Tokushima, 2-1, Minami-Josanjima, Tokushima, 770-8506
***Dr. of Eng., Associate Professor, The University of Tokushima, 2-1, Minami-Josanjima, Tokushima, 770-8506
****Technician, The University of Tokushima, 2-1, Minami-Josanjima, Tokushima, 770-8506

The aerodynamic stability of a Suramadu cable stayed bridge was investigated by a wind tunnel test. All tests in this study were carried out in smooth flow. Some fairings were examined to improve aerodynamic stability. The response characteristics of this model with the fairing were investigated by a spring supported sectional model. The visualization test was carried out to investigate the effect of the flow around the model on its aerodynamic stability. As the results of this study, it was indicated that the fairing hardly affects the flow below the model and the aerodynamic stability is controlled by the separation strength (vorticity) and the thickness of separation bubble above the model.

Keyword: improvement of aerodynamic stability, fairing, flow visualization

1. Introduction

Suramadu Bridge is now being constructed at East Java Island Indonesia, and scheduled to start its activity in 2008. This bridge on the Madura strait connects Madura Island with Java Island. Total length of the bridge is 5 km, including main bridge and approach bridges at both sides. The type of main bridge is a cable stayed bridge that has main span of 434 m and two side spans of 192 m. The deck has a 30 m width, supported by two box girders and is separated into two carriageways and two sidewalks by handrails.

Wind induced vibrations are primary consideration for the safety of long span bridges. Wind tunnel test is the most reliable technique to investigate the aerodynamic performance of bridge in strong wind. Generally, there are three kinds of bridge model test; full model test, sectional model test and taut strip model test, for the investigation of the aerodynamic characteristics of cable stayed bridge in wind tunnel test. Sectional model test is commonly used for identification of aerodynamic parameters. Scanlan and Tomko[1)] were one of the pioneers in the testing model of long span bridge.

Several studies concerning in the instability of box girder of long span bridge (Walshe and Wyatt[2)], Miyata et al.[3)], Kobayashi et al.[4)], Narita et al.[5)]) have been investigated. In these studies, some aspects of aerodynamic stability of bridge deck were carried out such as, vortex induced responses of cable stayed bridge, improvements of flutter stability, flow around surface model, pressure distribution and unsteady aerodynamic forces.

Aerodynamic stability is greatly affected by the shape of bridge deck section. There are some kinds of aerodynamic devices, which can improve the aerodynamic instability of bridge deck section, such as flap, edge plate, side plate and fairing. Triangular fairing is commonly used to improve the aerodynamic instability of the bridge deck. Nagao et al.[6)] investigated the effect of triangular fairings on the aerodynamic stability of two kinds of box girders whose thickness ratio, *B/H*, was different. In their study, it was concluded that the effective fairing shape for individual bridge section could be determined by flow properties around the individual bridge deck. Yoshimura et al.[7)] reported the effect of small triangular fairings. In their study, one type of the triangular fairing was effective in suppressing the aerodynamic oscillation. Daito et al.[8),9)] investigated the aerodynamic properties of two edge girders and their aerodynamic stability was improved by the inclination of lower flanges and the location of the edge girders. They pointed out that flow around lower surface played an important role on the aerodynamic stabilization of two edge girders.

In this study, the aerodynamic stability of the new bridge, Suramadu cable stayed bridge, was investigated by a spring supported sectional model and the effect of triangular fairings on the aerodynamic stability was also examined. Moreover, the visualization test of the flow around the model was carried out to investigate the effect of the fairings on the flow around the model.

2. Experimental Condition

The sectional model test was carried out in the Eiffel type of wind tunnel test at the University of Tokushima. The wind tunnel test has a working section of 0.7 m wide, 1.5 m high and 4 m long. The cross section of the prototype bridge for this test is shown in Figure 1. The bridge deck stiffened by two edge boxes and covered by RC slab with 0.25 m depth was stayed by multi-cables in two planes above the boxes. The reduced scale of 1/85 was chosen, giving a model width B = 0.35 m. The properties of structure are shown in Table 1.

The measurement of the aerodynamic responses of bending and torsional mode for sectional model was carried out, where the angle of attack α = -3°, 0° and +3°. The center of rotation was assumed at the location between the center of gravity and the shear center. The model with a length of 0.6 m and width of 0.35 m was suspended in eight coil springs to enable vertical and torsional motions. Wire systems were installed to constrain other motions such as lateral, longitudinal deflections and rotation about a vertical axis. The aspect ratio of model defined by the ratio of length to width is about 1.7 and the aspect ratio defined between length and depth is 15. However, the effect of aspect ratio of model should be ignored by the use of enough large end plates as shown in Photo 1. The wind tunnel test was carried out in smooth flow condition at wind speed up to 10 ms^{-1}. LabVIEW software was used to measure and analyze the data signal.

To improve the aerodynamic instability of the deck, some fairings shown in Table 2 were examined. The angle of elevation of lower surface of fairing was changed from 30° to 60°, where 44° was coincide with the angle of elevation of the deck as shown in Figure 2. First two digits of fairing name is the angle of elevation of lower surface and last two digits expresses the angle of depression of upper surface.

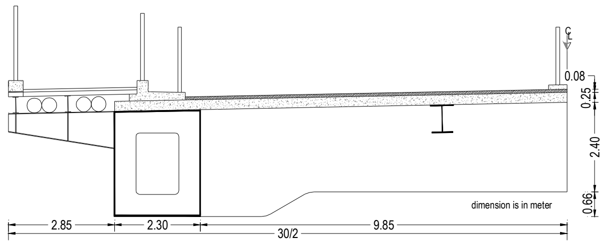

Figure 1 Cross section of the bridge

Photo 1 Sectional model

Table 1 Structural properties of prototype and model

Properties	prototype	model	
		required	measured
width (m)	30	0.353	0.35
depth (m)	3.64	0.042	0.04
equivalent mass (kg/m)	35,212	4.873	4.958
center of rotation from bottom surface (m)	(3.07)		0.030
mass of moment inertia (kg m^2/m)	2,097,466	0.040	0.039
bending natural frequency f_η (Hz)	0.39	3.596	2.977
torsional natural frequency f_ϕ (Hz)	0.54	4.979	4.094
f_ϕ/f_η	1.385	1.385	1.375
Logarithmic damping δ_ϕ (2ϕ = 1°) δ_ϕ (2ϕ = 2°)			0.008 0.012
Logarithmic damping δ_η ($2\eta/B$ = 0.03)			0.009

In order to clarify the aerodynamic properties of the bridge deck in detail, structural damping of model was set to smaller value than that of estimated prototype deck.

Table 2 Type of fairing (mm)

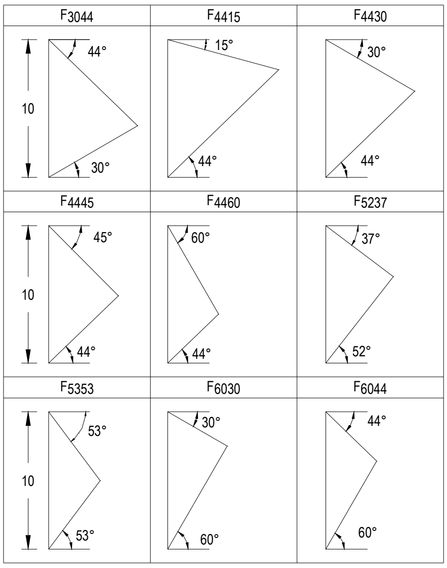

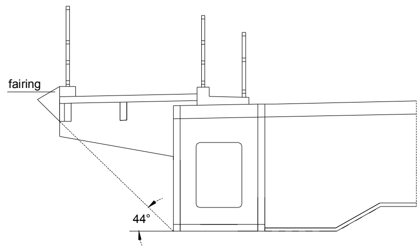

Figure 2. Fairing position

The smoke wire method was used to visualize the flow surrounding the model under forced vibration. A stainless steel wire with diameter 0.1 mm coated with liquid paraffin was placed at the upstream of the model. The stainless steel wire was heated by using an electric current and white smoke was then appearing into the flow. The flow patterns around surface of model were recorded using a high speed camera (100 frames/s). The amplitude of oscillation for torsional mode (2ϕ) was 2° and reduced wind velocity (U/fB) were 3, 4 and 5, where wind velocity ,U, was fixed to 1 m/s for all cases.

3. Result and analysis

3.1. Aerodynamic damping

Figure 3 shows the aerodynamic damping of torsional vibration at specified double amplitude, 2ϕ=2°, under the angle of attack, α=3°, as the function of reduced wind velocity. In this figure, the maximum damping, reduced wind velocity appearing the maximum damping and reduced wind velocity at zero cross indicate the stability of the model. The result of F4460 shows almost the same as that of WOF (basic section model without fairing). On the other hand, in the result of fairing F4430 was the most stable and has a possibility of flutter appearance in the higher reduced wind velocity.

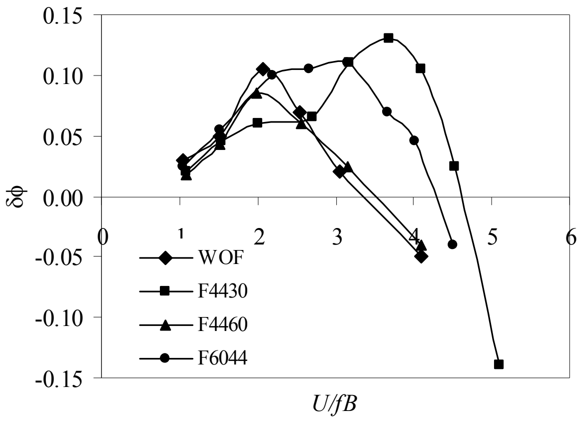

Figure 3 Aerodynamic damping (2ϕ= 2^o, α=3^o)

3.2 Aerodynamic responses

For all sections tested here, aerodynamic properties of vertical bending mode were quite stable. The aerodynamic stability of two edge box girder deck section decreased in positive angle of attack as same as the result obtained in previous research[8]. In the case of α=-3 ^{o}, there was no oscillation and more stable results were obtained in α=0^o in comparison with those in α=+3^o.

Figure 4 shows the chart of double torsional amplitude of the model, 2ϕ, to reduced wind velocity, *U/fB*, for all fairings at α=+3^o. The line entitled "WOH" represents the result of the model without handrail. From the comparison of the critical flutter speed between WOH and WOF, the handrail reduces the flutter speeds about 10%. For the basic section, WOF, vortex induced oscillation and torsional flutter were observed. In the vortex induced oscillation region, minimum aerodynamic damping measured in the wind tunnel test was $\delta_{\phi aero}$=-0.0075, which was enough small in comparison with the estimated structural damping of prototype bridge, δ_ϕ=0.02. Therefore, the vortex induced oscillation of the prototype bridge should be disappeared. Referring to this figure, F4415, F4445, F4460, F3044, F6030 and F5353 show a little increase of flutter speed. On the other hand, the flutter speeds for F4430, F6044 and F5237 were as high as 30% of that of WOF.

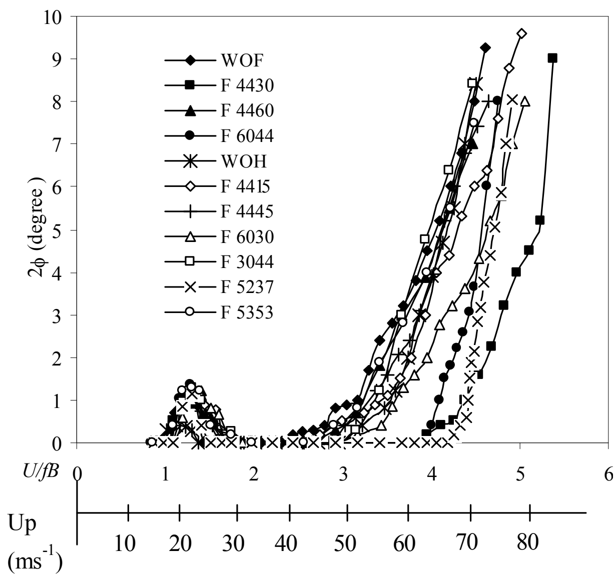

Figure 4 Aerodynamic responses at α= +3^o

Critical flutter speeds with fairing models that had the same angle of elevation of lower surface of fairing and the different angle of depression of upper surface did not coincide each other. Moreover, critical flutter speeds with fairing models that had the different angle of elevation of lower surface of fairing and the same angle of depression of upper surface were also different. The representative parameters of the fairing shape are the position of the fairing tip and tip angle. Figure 5 (a), (b) and (c) show the effect of the nondimensional height of fairing tip, H_e/H_f, that of the nondimensional length of it, L_e/H_f, and that of fairing tip angle on flutter speed, respectively. For this cross section, the flutter speed has a sharp peak around H_e/H_f=0.62. On the contrary, flutter speeds are no relation between L_e/H_f and tip angle, α_e, respectively.

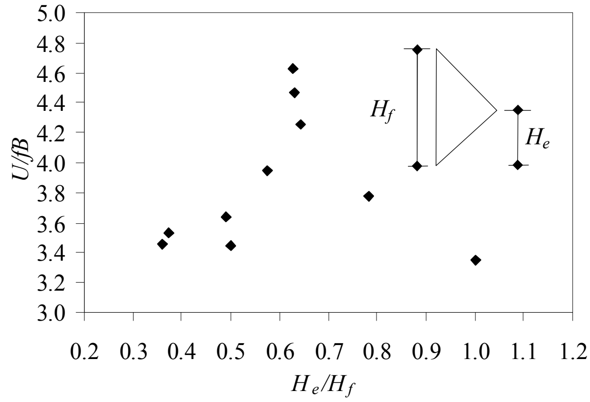

Figure 5(a) Flutter speed v.s. Ratio of the height of fairing tip to the depth of fairing

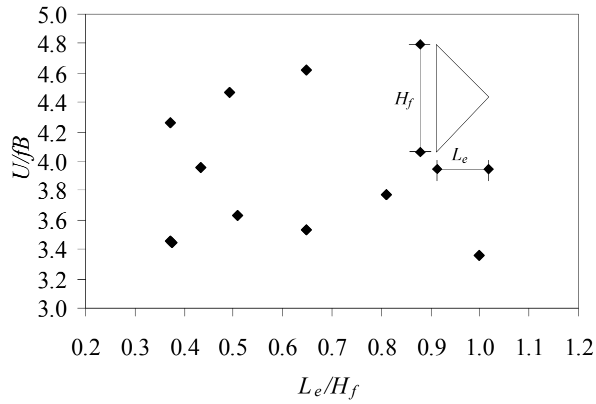

Figure 5(b) Flutter speed v.s. Ratio of the width of fairing tip to the depth of fairing

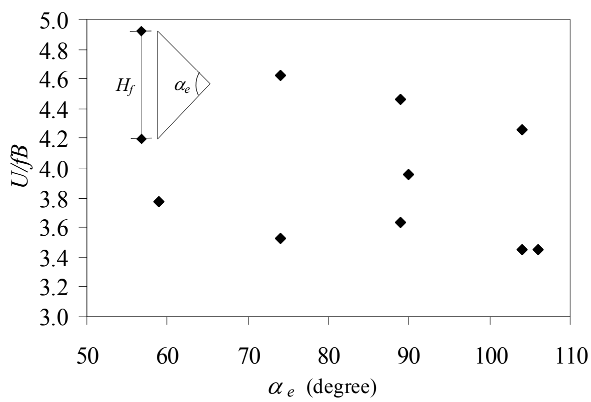

Figure 5(c) Flutter speed v.s. Angle of fairing tip

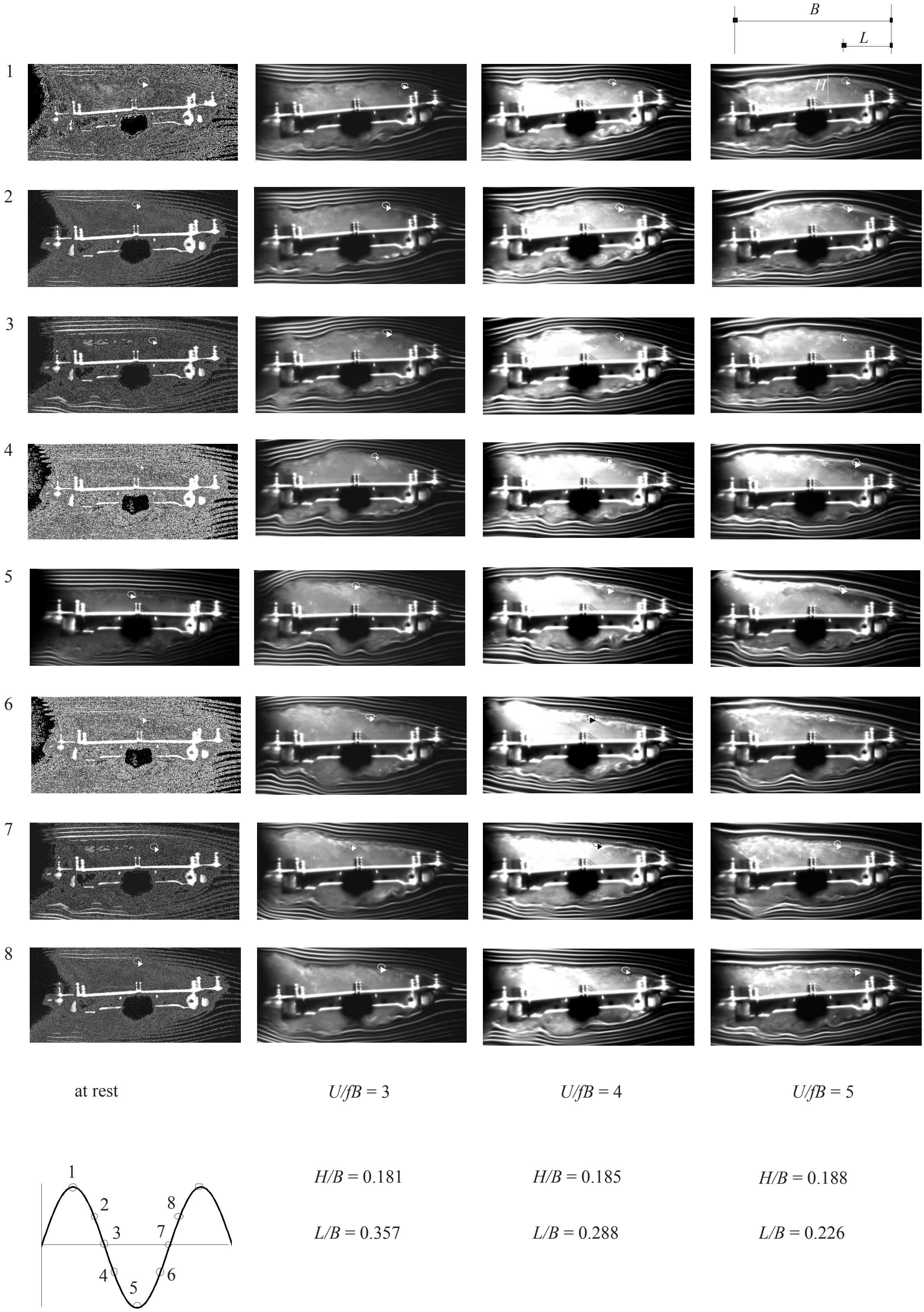

Figure 6 Instantaneous flows around the model without fairing (WOF)

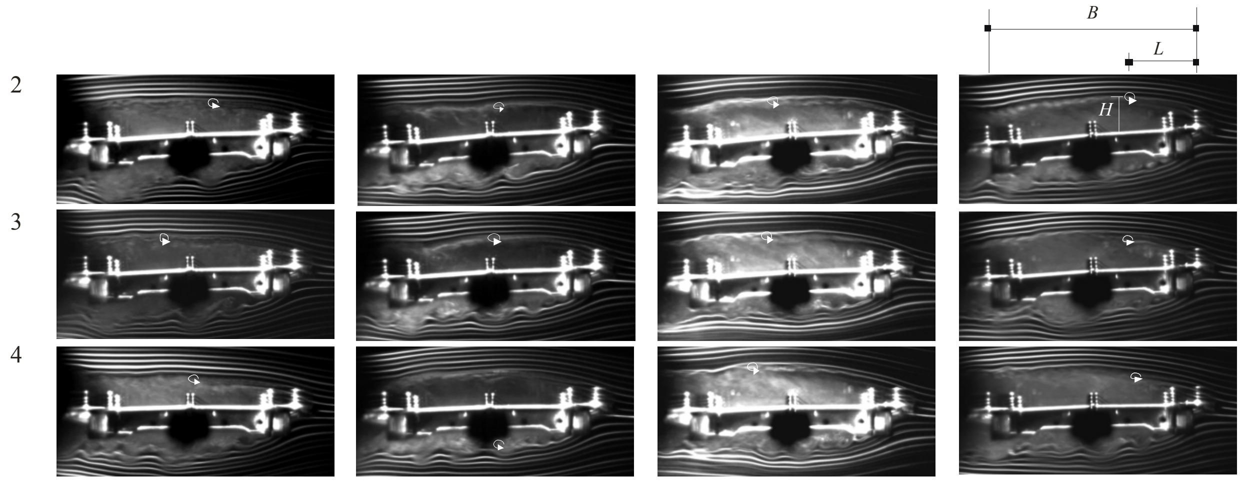

at rest | $U/fB = 3$ | $U/fB = 4$ | $U/fB = 5$

$H/B = 0.164$ | $H/B = 0.167$ | $H/B = 0.169$

$L/B = 0.536$ | $L/B = 0.525$ | $L/B = 0.360$

(a) flows around F44 30

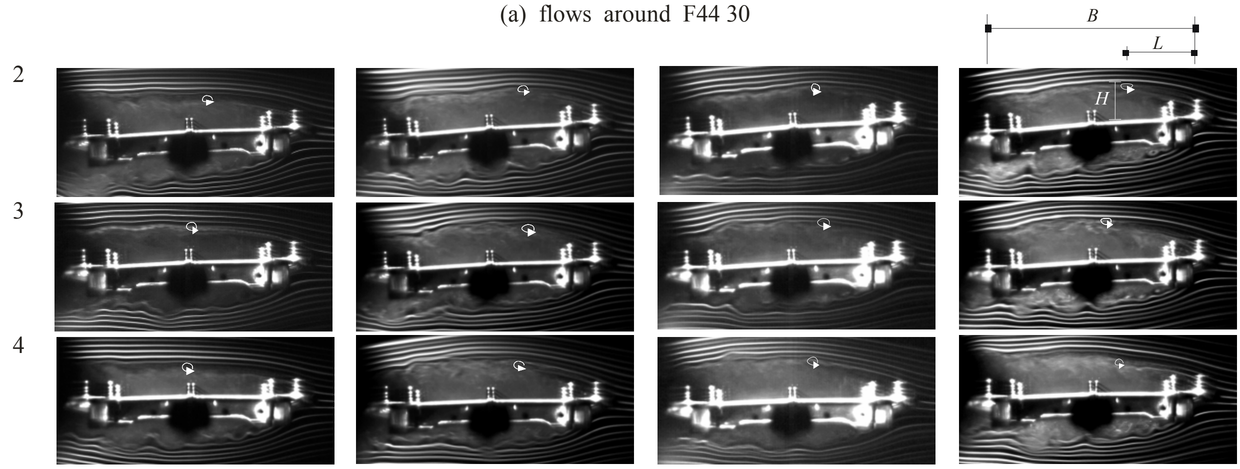

at rest | $U/fB = 3$ | $U/fB = 4$ | $U/fB = 5$

$H/B = 0.174$ | $H/B = 0.177$ | $H/B = 0.181$

$L/B = 0.396$ | $L/B = 0.355$ | $L/B = 0.285$

(b) flows around F44 60

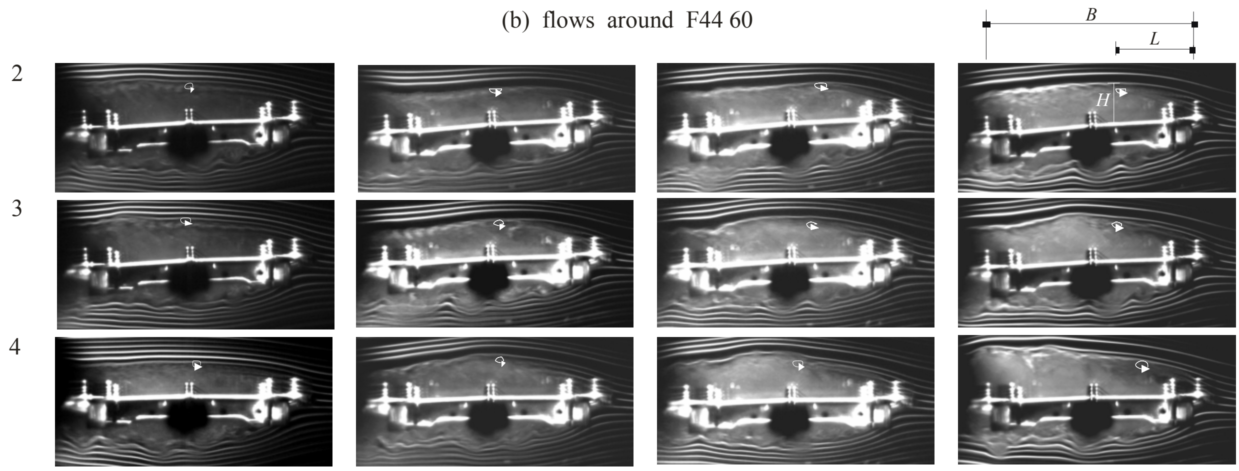

at rest | $U/fB = 3$ | $U/fB = 4$ | $U/fB = 5$

$H/B = 0.173$ | $H/B = 0.177$ | $H/B = 0.180$

$L/B = 0.503$ | $L/B = 0.476$ | $L/B = 0.353$

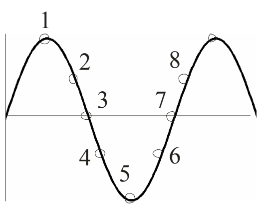

(c) flows around F6044

Figure 7 Instantaneous flows around the model with fairing

3.3. Flow visualization test

Figures 6 and 7 show the flows around the model at each phase in one time cycle of torsional motion with $2\phi=2^o$, $\alpha=+3^o$, *U/fB*=3, 4, 5 are indicated for WOF, F4430, F4460, and F6044, respectively. Furthermore, the photographs entitled "at rest" represent the flow around the model, where the angle of attack is set to the same with the instantaneous angle of attack for each phase. The circular arrow in these figures indicates the most outside point where two adjacent smoke lines unified. It is supposed that this point relates to the formation of separated bubble. *L* is the distance from the leading edge to the circular arrow. *H* is the depth of the separation bubble at the point of 0.4*B* from the leading edge. Actually the height of separation flow is variable along the width of bridge deck (*B*) and each phase angle. The value of 0.4 *B* was chosen for the representative point of reference to calculate the height of separation flow, because the point of 0.4*B* always presents in all figures. Referring to these figures, the separation flow below the model for all conditions is very similar, because the separation flow below the model is controlled by the edge of the box girder. Therefore, the fairing hardly affects the flow below the model. In order to modify the flow around lower surface, the change of location of two girders or the inclination of lower flanges was necessary, as pointed out by Daito et al[8),9)]. The separation flow above the model is different each other.

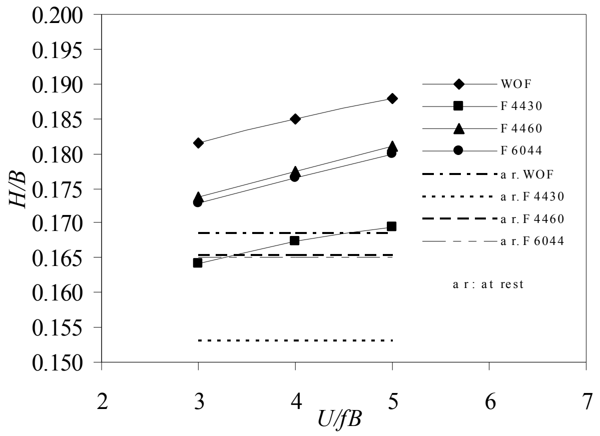

Figure 8 Ratio *H/B* to reduced wind velocity

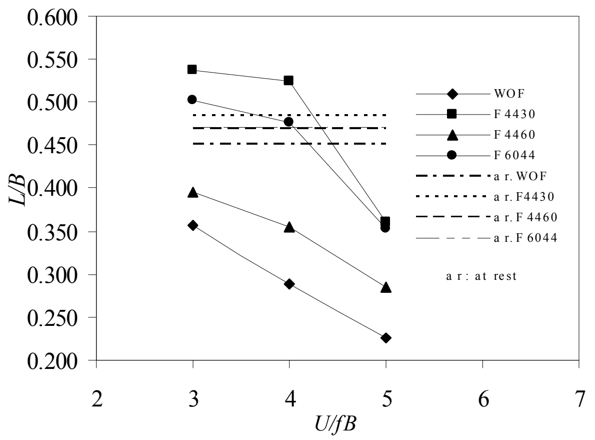

Figure 9 Ratio *L/B* to reduced wind velocity

Figures 8 and 9 show the *L/B* and *H/B* averaged for one cycle of the motion. *L/B* became larger in the order of WOF, F4460, F6044 and F4430, and *H/B* decreased in the same order. Moreover, the ratio *L/B* decreased with increasing the reduced wind velocity, on the other hand, the ratio *H/B* increased with increasing the reduced wind velocity. Therefore, for the aerodynamic unstable condition, *L/B* and *H/B* became smaller and larger, respectively. In the other word, the decrease of *L/B* and the increase of *H/B* indicate the increase of separation strength. It is considered that the behaviors of *L/B* and *H/B* reflect the unstability of flutter. It also shows good agreement with the results of the aerodynamic response.

4. Conclusion

The results of the study are summarized as follows:

1) Some fairings improve the flutter instability of Suramadu bridge successfully.
2) The fairing does not affect the flow below the model.
3) The fairing controls the flow above the model.
4) The effective fairing reduces the strength of separation flow above the model.

In order to clarify the effect of fairings on the flutter instability, unsteady pressure and unsteady aerodynamic forces should be investigated.

Acknowledgement

Authors express sincere thanks to Prof. Y. Kubo and co-workers of Kyushu Institute of Technology for kind advice on the flow visualization technique.

References

1) Scanlan,R.H. and Tomko,J.J., Airfoil and bridge deck flutter derivative, J. Eng. Mech. Div., Vol. 97 (EM6), pp.1717-1737, 1971.
2) Walshe,D.E. and Wyatt, T.A., Measurement and application of the aerodynamic admittance functions for a box girder bridge., J. Wind Eng. Ind. Aerodyn., Vol. 14, pp. 211-222, 1983.
3) Miyata,T., Miyazaki,M. and Yamada,H., Pressure distribution measurements for wind induced vibration of box girder bridges., J. Wind Eng. Ind. Aerodyn., Vol. 14, pp. 223-234, 1983.
4) Kobayashi,H., Bienkiewicz,B. and Cermak,E., Mechanism of vortex excited oscillations of a bridge deck., J. Wind Eng. Ind. Aerodyn., Vol. 29, pp. 371-378, 1988.
5) Narita,N., Yokoyama,K., Sato,H. and Nakagami,K., Aerodynamic characteristics of continuous box girder bridges relevant to their vibrations in wind., J. Wind Eng. Ind. Aerodyn., Vol. 29, pp. 399-408, 1988.
6) Nagao,F., Utsunomiya,H., Oryu,T. and Manabe,S., Aerodynamic efficiency of triangular fairing on box girder bridge., J. Wind Eng. Ind. Aerodyn., Vol. 49, pp. 565-574, 1993.
7) Yoshimura,T., Mizuta,Y., Yamada,F., Umezaki,H., Shinohara,T., Machida,N., Tanaka,T. and Harada,T., Prediction of vortex induced oscillation of a bridge girder with span wise varying geometry., J. Wind Eng. Ind. Aerodyn., Vol. 89, pp. 1717-1728, 2001.

8) Daito,Y., Matsumoto,M. and Takeuchi,T., Aerodynamic stabilization for geometrical girder shape of two edge girders of long span cable stayed bridges., Proc. 18th National Symposium on Wind Eng., pp. 431-436, 2004 (in Japanese).
9) Daito,Y., Matsumoto,M., Shirato,H., Yagi,T. and Takeuchi,T., Aerodynamic characteristics for stabilized section with two edge girders of long span cable stayed bridges., Proc. 19th National Symposium on Wind Eng. pp. 423-428, 2006 (in Japanese).

(Received September 18, 2007)